Synthesis of manganese dioxide/poly(3,4-ethylenedioxythiophene) core/sheath nanowires by galvanic displacement reaction

Kwang-Heon Kim · Ji-Young Kim · Kwang-Bum Kim

Abstract This paper describes a simple approach to prepare manganese dioxide/poly(3,4-ethylenedioxythiophene) (MnO_2/PEDOT) core/sheath nanowires with a controlled sheath thickness in the range of 2–10 nm. The PEDOT coating on a MnO_2 nanowire was performed by immersing the nanowires in an acidic solution containing 3,4-ethylenedioxythiophene (EDOT) monomers. Analysis of open-circuit potential of the MnO_2 nanowire electrode in the solution indicates that a galvanic displacement reaction between MnO_2 and EDOT is responsible for the synthesis of the MnO_2/PEDOT core/sheath nanowire.

1 Introduction

One-dimensional (1-D) nanostructures such as nanorods, nanowires, nanotubes, and nanobelts have been intensively investigated in recent years due to their potential applications in fabricating nanoscale electronic, sensing, and energy conversion and storage devices [1]. In particular, 1-D nanostructured metal oxides have become key components in energy conversion and storage devices owing to their large aspect and surface-to-volume ratios, which can dramatically increase their effective surface area and, thus, enhance their size-related properties [2–4]. Recently, 1-D core/sheath nanowires have attracted interests as another type of 1-D nanostructures because their functions could be further enhanced by fabricating the core and sheath from different materials [5].

1-D manganese dioxide (MnO_2) nanowire has been reported as a promising electroactive material for energy storage devices because of its high energy density, low cost, and natural abundance. However, its poor electronic conductivity needs to be improved to enhance the electrochemical properties [6, 7]. Poly(3,4-ethylenedioxythiophene) (PEDOT) is a most promising conducting polymer due to its high electrical conductivity (~600 Scm^{-1}) and good environmental stability among other polymers [8]. Synthesis of MnO_2 core and PEDOT sheath nanowire would exhibit a synergy effect on the electrical, electrochemical, and mechanical properties for energy storage device applications.

Chemical polymerization of monomers using a soluble oxidizing agent has been reported for the preparation of conducting polymer coated metal oxides [9, 10]. However, it is difficult to control the morphology and thickness of conducting polymers on the nanometer scale. Furthermore, it is highly likely to produce a separate free polymer particles away from the oxide as well as a partial coating of polymer on the surface of a metal oxide.

Previously, chemical oxidation of pyrrole into polypyrrole in the presence of α-MnO_2, β-MnO_2 or spinel $LiMn_2O_4$ was reported by injecting a liquid pyrrole into an acidic medium containing suspended manganese oxide without using any soluble oxidizing agents. Gemeay et al. reported on the preparation of PANI/MnO_2 composite by using β-MnO_2 as an oxidant in an aniline solution [11]. In their study, β-MnO_2 micro-rods transformed PANI/MnO_2 composite with a morphological change to a particulate cluster and a crystallographic phase change to an amorphous phase during the polymerization. Furthermore, free PANI particles were observed in the cluster. In principle, PANI should be

K.-H. Kim · J.-Y. Kim · K.-B. Kim (✉)
Department of Material Science and Engineering,
Yonsei University,
134 Shinchon-dong, Seodaemoon-gu,
Seoul 120-749, South Korea
e-mail: kbkim@yonsei.ac.kr

prepared as a thin layer on MnO_2 template to make a PANI/MnO_2 core/sheath without causing any change in the morphology and crystallographic phase of MnO_2.

Galvanic displacement reaction is a spontaneous process which involves the reduction of ions of a more noble metal along with a simultaneous oxidation of a less noble metal driven by a difference in redox potentials of two redox couples. It has been extensively used for the synthesis of Co/Au core/sheath nanoparticles [12] and Cu_2S/Au core/sheath nanowires [13] in which the metallic core was used as a reducing agent as well as a sacrificial template. The chemical polymerization using a sacrificial oxide could be considered as a galvanic displacement reaction since it is driven by a difference in redox potentials of two redox couples. Analysis of the galvanic displacement reaction for the synthesis of metallic core/sheath nanostructures would offer an insight into the synthesis of metal oxide/conducting core/sheath nanostructures as well.

In this study, open-circuit potential (OCP) of a MnO_2 nanowire electrode was monitored to investigate the oxidative polymerization of EDOT monomers on the MnO_2 nanowire from the view of the galvanic displacement reaction. We report on the synthesis of a MnO_2/PEDOT core/sheath nanowire with a controlled sheath thickness without using additional soluble oxidizing agents.

2 Experimental

MnO_2 nanowires were prepared by a redox reaction of MnO_4^- and Mn^{2+} in an aqueous solution according to the following reaction: $2MnO_4^- + 3Mn^{2+} + 2H_2O \rightarrow 5MnO_2 + 4 H^+$ [14]. In a typical synthesis, a mixture of 40 ml of 0.1 M $KMnO_4$ solution and 60 ml of 0.1 M $MnSO_4$ solution were refluxed at 90 °C for 12 h. A dark-brown precipitate was repeatedly washed with deionized water, centrifuged, and dried at 100 °C in air for 12 h.

For PEDOT coating, 0.1 g of MnO_2 nanowires were added into 40 ml of 0.01 M EDOT (Aldrich) aqueous solution under stirring. Then, 2 ml of 1 M H_2SO_4 solution was added and the solution was stirred for 1 h. For comparison, a pure PEDOT was prepared on a Ni substrate by an electrochemical polymerization using potential cycling in a solution of 0.01 M EDOT and 0.025 M $LiClO_4$.

The MnO_2 nanowires electrode was prepared onto a Pt coated Si wafer by an electrostatic spray deposition (ESD) technique for the OCP measurements. The procedure of making an electrode using the ESD has been described in detail elsewhere [15]. The OCP measurements were performed in a two-electrode cell using a potentiostat/galvanostat (VMP2, Princeton Applied Research). The working and reference electrode were the MnO_2 nanowires electrode and saturated calomel electrode (SCE), respectively.

X-ray diffraction (XRD) measurements were carried out with a Regaku Rint-2000 instrument using Cu-Kα radiation (λ=1.54178 Å). Raman spectra were measured on a Jobin-Yvon T64000 spectrophotometer (excitation radiation= 514.532 nm). The morphology was examined by transmission electron microscopy (TEM, JEOL JEM2100F) and scanning electron microscope (SEM, Hitachi S-4300SE).

3 Results and discussion

Scheme 1 illustrates the schematics for the synthesis of the MnO_2/PEDOT core/sheath nanowires. When MnO_2 nanowires are immersed into an acidic solution containing the EDOT monomers, the surface layer of MnO_2 nanowires is spontaneously displaced with a thin layer of PEDOT, because of an oxidative polymerization of EDOT on the surface of MnO_2 driven by a reduction of Mn^{4+} of the MnO_2 nanowire to soluble Mn^{2+} ions due to a difference in the redox potentials of MnO_2/Mn^{2+} ($E°$=1.2 V_{SHE}) [16] and EDOT/PEDOT ($E°$=1.0 V_{SHE}) [17].

To monitor the reaction, the OCP of the MnO_2 nanowire electrode was measured in an acidic solution containing EDOT monomers. The OCP indicates a redox state at an interface between the MnO_2 nanowire and the solution. By monitoring of the OCP, oxidation reaction of the EDOT and reduction reaction of the MnO_2 can be observed.

Figure 1 shows the change in the OCP of the MnO_2 electrode during the synthesis of MnO_2/PEDOT core/sheath nanowires. The OCP indicates a redox state of the MnO_2 nanowire in contact with the solution. Considering the change of the OCP as a function of time, there are three distinct stages of S1, S2, and S3 in the OCP-time profile.

Initially, the OCP of the MnO_2 electrode in contact with the solution was measured to be 0.3 V. Upon the dropwise addition of 1 M H_2SO_4, the potential instantly jumped to 0.89 V due to a rapid decrease in pH in the first stage (S1) [16]. Right after the sharp increase in OCP, it rapidly dropped to 0.85 V and then remained a potential plateau around 0.85 V in the second stage (S2). This value of the potential plateau is similar to that observed for an electrochemical polymerization of EDOT using galvanostatic technique [18]. It suggests that the reaction occurring at 0.85 V might be associated with an oxidative polymerization of EDOT and a simultaneous reduction of MnO_2. As the reaction proceeded in the second stage for 30 min, dark-brown MnO_2 turned to deep-blue indicating the formation of PEDOT on the MnO_2 nanowires.

For comparison purposes, the OCP of the MnO_2 nanowire electrode was measured also measured in an acidic solution without EDOT and in a neutral solution with EDOT. It was 0.95 V (Fig. 1, inset (a)) and 0.3 V (Fig. 1, inset (b)), respectively. Little variation of the OCP was

Scheme 1 Schematic of the process for the synthesis of MnO$_2$/PEDOT core/sheath nanowires
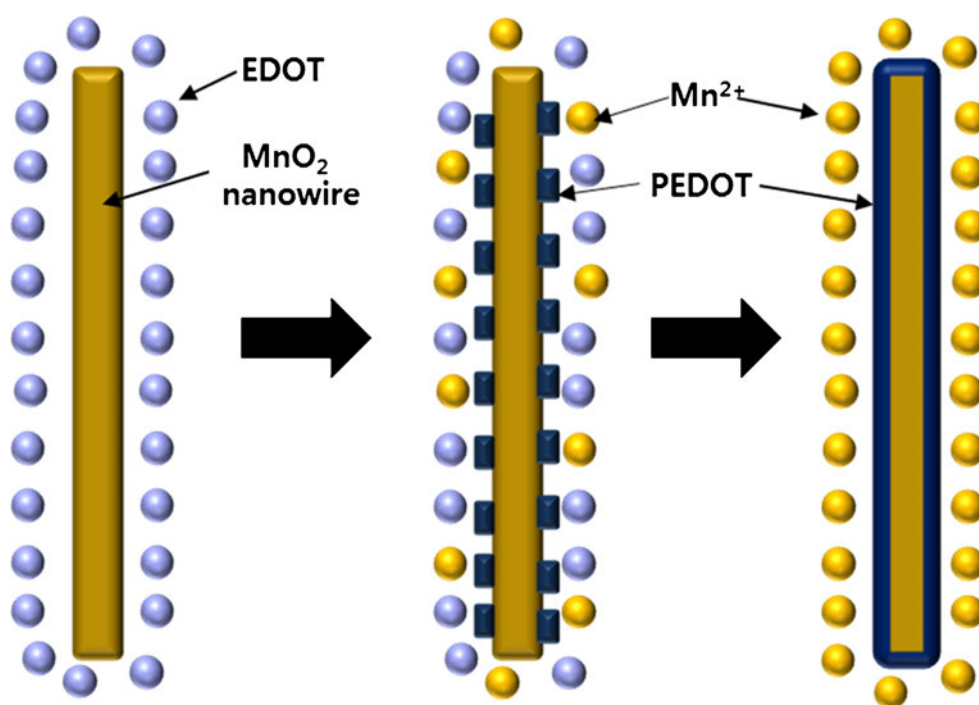

observed with time in either case. It indicates no chemical reaction occurred between the MnO$_2$ electrode and the EDOT solution

In the third stage (S3), the OCP decreased rapidly to 0.45 V and then approached to 0.4 V, which is close to the OCP of a pure PEDOT electrode in an acidic solution. As

the surface of MnO$_2$ nanowires became covered by the PEDOT layer via the galvanic displacement reaction, the electrode/solution interface changed from MnO$_2$/solution to PEDOT/solution, lost the driving force for the galvanic displacement reaction and showed the OCP of PEDOT in an acidic solution. . Analysis of Fig. 1 suggests the galvanic

Fig. 1 OCP of the MnO$_2$ nanowire electrode measured in 0.01 M EDOT as a function of time (inset: MnO$_2$ nanowire electrode (**a**) in an acidic solution without EDOT and (**b**) in a neutral solution with EDOT)
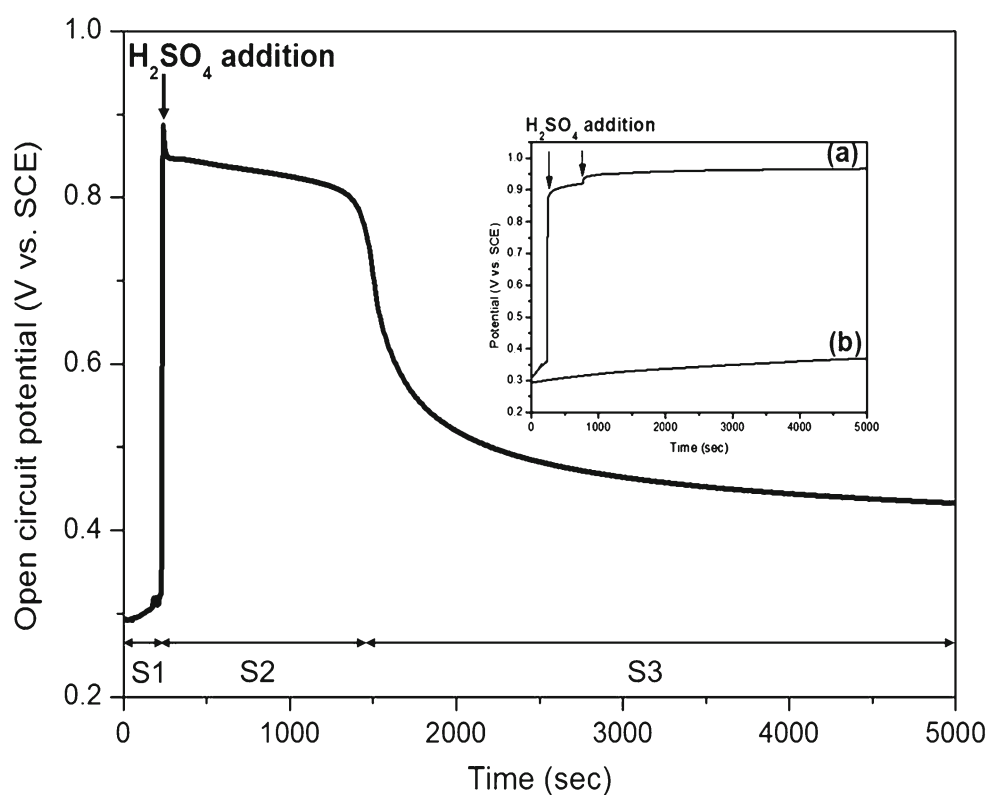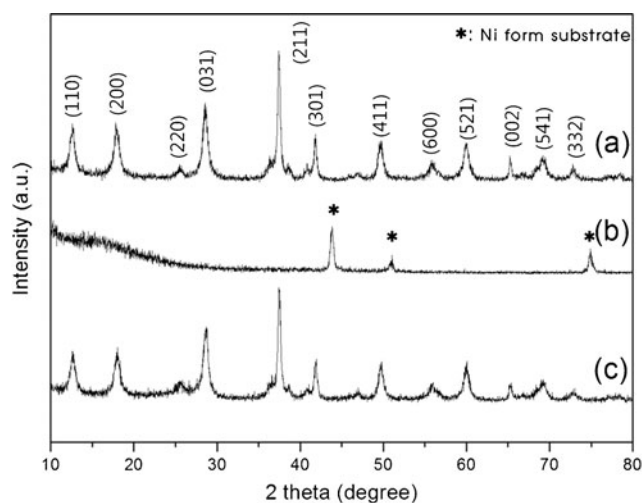
Fig. 2 XRD patterns of (**a**) MnO_2 nanowires, and (**b**) MnO_2/PEDOT core/sheath nanowires

displacement reaction taking place between MnO_2 and EDOT in an acidic solution due to the difference in the redox potentials of two materials.

During the galvanic displacement reaction, MnO_2 might be reduced with a formation of Mn_2O_3, MnOOH, Mn_3O_4 and $Mn(OH)_2$ [19]. XRD measurements were carried out in order to investigate the structure stability of MnO_2 nanowires during the galvanic displacement reaction. Figure 2 shows the XRD patterns of the MnO_2 nanowires, PEDOT, and MnO_2/PEDOT core/sheath nanowires, respectively. As shown in Fig. 2(a), all the XRD pattern of MnO_2 nanowires can be exclusively indexed as a tetragonal α-MnO_2 (JCPDS 44-0141). The pure PEDOT prepared by electrochemical polymerization does not yield any characteristic peaks, indicating the amorphous nature of polymer as shown in Fig. 2(b). After the PEDOT coating, the original crystal structure of α-MnO_2 nanowires was maintained and no reduced phases such as Mn_2O_3, MnOOH Mn_3O_4, and $Mn(OH)_2$ were found in the XRD pattern in Fig. 2(c). However, there were no PEDOT diffraction peaks of the MnO_2/PEDOT core/sheath nanowires due to the amorphous nature of PEDOT.

To further examine the PEDOT in the MnO_2/PEDOT core/sheath nanowires, Raman spectroscopic studies were conducted. Figure 3 shows the Raman spectra of the the MnO_2 nanowires, MnO_2/PEDOT core/sheath nanowires, and PEDOT, respectively. The Raman spectrum of the MnO_2 (Fig. 3(a)) is dominated by two bands at 583 and 642 cm^{-1}, respectively. This feature is close to that of a cryptomelane-type MnO_2 [20]. Raman spectrum of the PEDOT/MnO_2 clearly shows the characteristic bands at 1439 cm^{-1} is assigned to the symmetric stretching mode of the aromatic C = C band, while a less intense band at 1504 cm^{-1} is attributed to the C = C antisymmetric stretching vibration. Other, weaker bands at 1367 and 1253 cm^{-1} are assigned to the stretching mode of the single C-C bond

and the C-C inter-ring bond, respectively (Fig. 3(b)) [21]. This feature is similar to that of the PEDOT shown in Fig. 3 (c), which indicates the presence PEDOT in the composite nanowires. Although no obvious PEDOT diffraction peaks could be observed from XRD analysis of the MnO_2/PEDOT core/sheath nanowires, Raman spectrum in Fig. 3(b) clearly shows the presence PEDOT in the composite nanowires. Analysis of the XRD and Raman spectra indicates that the galvanic displacement reaction between MnO_2 and EDOT did not cause any phase transformation of MnO_2.

SEM images shown in Fig. 4 represent the typical MnO_2 nanowires and the MnO_2/PEDOT core/sheath nanowires synthesized in this study. The SEM image of the MnO_2 nanowires shows the well-dispersed individual nanowires with 40–50 nm in diameter and length up to 3 μm (Fig. 4 (a)). After the PEDOT coating on the MnO_2 nanowire, diameter of MnO_2 nanowires increased up to 50–60 nm (Fig. 4(b)). It should be noted that no free PEDOT particles were found as expected from the view of reaction mechanism of the galvanic displacement reaction used to prepare the MnO_2/PEDOT core/sheath nanowires.

TEM was employed to investigate the morphological feature of the core/sheath nanowires. Figure 5(a) shows a HRTEM image of the as-prepared MnO_2 nanowires with ~40 nm in diameter before PEDOT coating. Figure 5(b–d) show HRTEM images of the MnO_2/PEDOT core/sheath nanowires prepared by the galvanic displacement reaction for different reaction time. At 300 s, only 2 nm PEDOT coating was formed on the MnO_2 nanowire. This thin layer of PEDOT was relatively rough but seemed to be continuous along this nanowire. As coating proceeded, the PEDOT sheath became thicker, smoother, and more uniform (Fig. 5(c and d)). A sharp contrast between the outer PEDOT layer and the inner MnO_2 wire indicates a core/sheath structure of the composite nanowire.
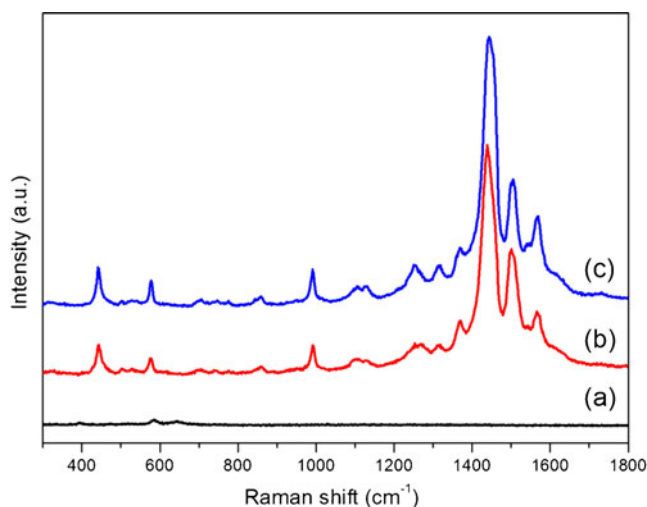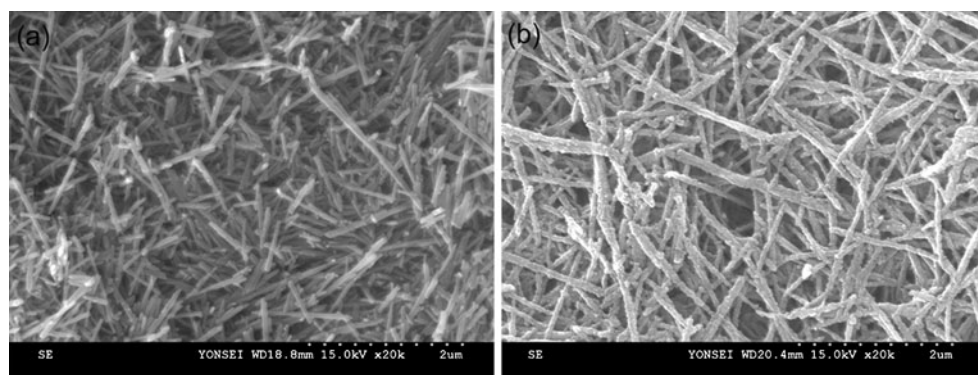

Fig. 3 Raman spectra of (**a**) MnO_2 nanowires, (**b**) MnO_2/PEDOT core/sheath nanowires and (**c**) pure PEDOT

Fig. 4 SEM images of (**a**) MnO$_2$, and (**b**) MnO$_2$/PEDOT core/sheath nanowires

As the PEDOT coating time was increased, it is clearly seen that the PEDOT coating thickness increased, however, the diameter of the MnO$_2$ nanowire decreased. It is due to the galvanic displacement reaction in which the surface layer of MnO$_2$ nanowires were partially reduced into dissolvable Mn^{2+} ions and simultaneously EDOT monomers were oxidized to PEDOT layer on the surface of MnO$_2$ nanowires according to the following galvanic
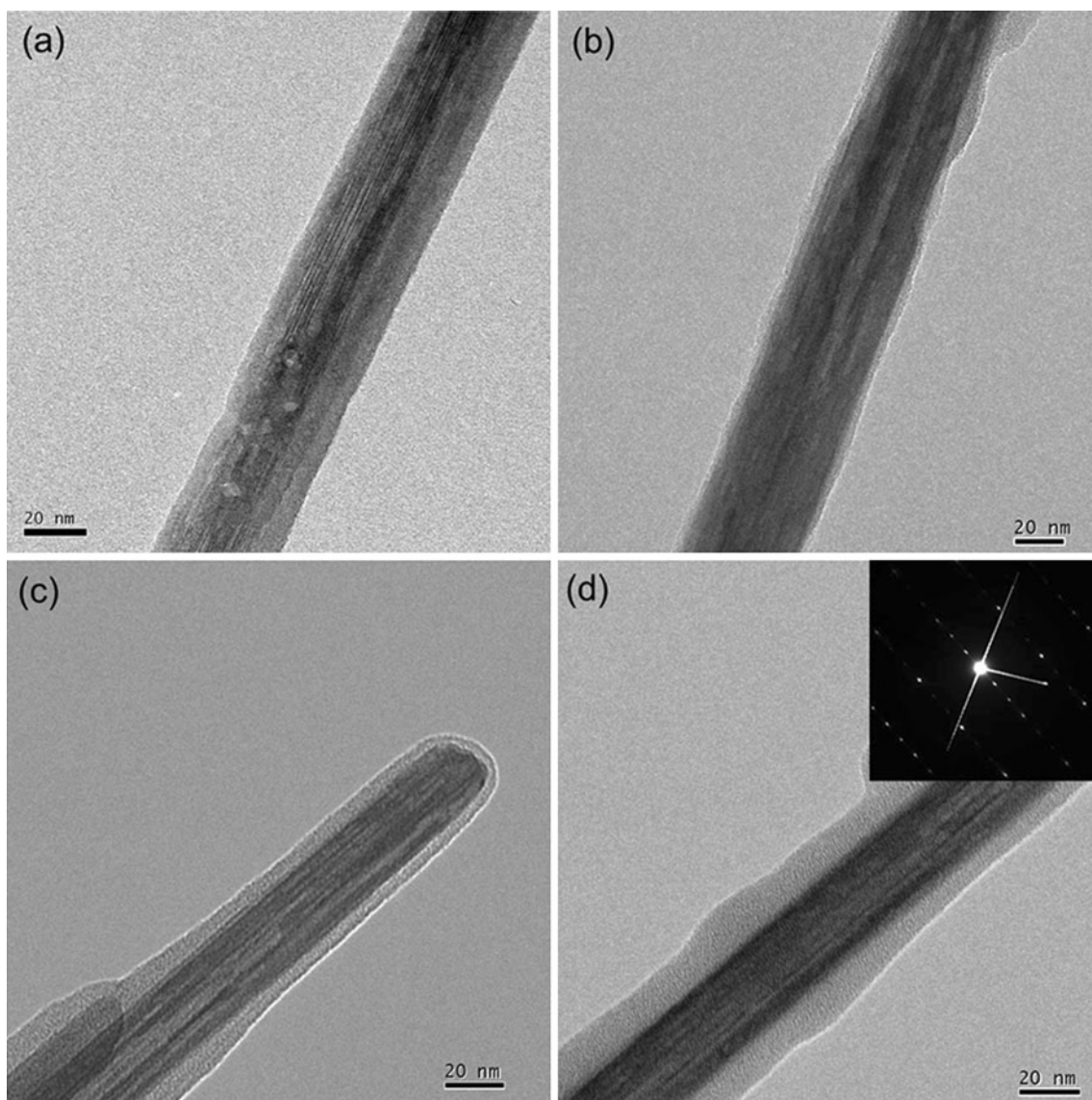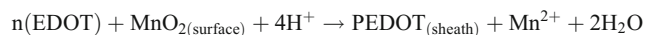

Fig. 5 TEM images of (**a**) MnO$_2$ nanowires, MnO$_2$/PEDOT core/sheath nanowires obtained after the PEDOT coating for (**a**) 300 s, (**b**) 600 s, and (**c**) 1200 s

displacement reaction:

$$n(EDOT) + MnO_{2(surface)} + 4H^+ \rightarrow PEDOT_{(sheath)} + Mn^{2+} + 2H_2O$$

The selected area electron diffraction patterns of the single MnO_2/PEDOT core/sheath nanowire (inset in Fig. 5(d)) are consistent with the single crystalline nature of a bulk sample, and can be indexed to the reflections of tetragonal α-MnO_2 [1$\bar{1}$1]. These results indicate that the PEDOT coating process by galvanic displacement reaction did not change in the morphology and crystallographic phase of α-MnO_2.

This study demonstrates that the MnO_2/PEDOT core/sheath nanowires could be prepared to have a continuous layer of PEDOT with a uniform thickness on the 1-D MnO_2 wire on the nm scale using the galvanic displacement reaction.

4 Conclusions

We demonstrate that the MnO_2/PEDOT core/sheath nanowires could be prepared to have a continuous layer of PEDOT with a uniform thickness on the 1-D MnO_2 wire on the nm scale using the galvanic displacement reaction by immersing the MnO_2 nanowire in an acidic aqueous solution containing EDOT monomers without using any additional soluble oxidizing agents. Analysis of the OCP of the MnO_2 nanowire electrode in the solution containing EDOT monomers indicates that a galvanic displacement reaction between MnO_2 and EDOT, which involves a reduction of Mn^{4+} of the MnO_2 nanowire to soluble Mn^{2+} ions and simultaneous oxidation of the EDOT monomers to PEDOT on the surface of MnO_2 nanowires, is responsible for the synthesis of the MnO_2/PEDOT core/sheath nanowire.

References

1. Y. Xia, P. Yang, Y. Sun, Y. Wu, B. Mayers, B. Gates, Y. Yin, F. Kim, H. Yan, Adv. Mater. **15**, 353 (2003)
2. Y. Zhang, K. Suenaga, C. Colliex, S. Iijima, Science **281**, 973 (1998)
3. J. Liu, G. Cao, Z. Yang, D. Wang, D. Dubois, X. Zhou, G.L. Graff, L.R. Pederson, J.G. Zhang, ChemSusChem **1**, 676 (2008)
4. L.J. Lauhon, M.S. Gudiksen, D. Wang, C.M. Lieber, Nature **420**, 57 (2002)
5. Y.D. Yin, Y. Lu, Y.G. Sun, Y.N. Xia, Nano Lett. **427** (2002)
6. B.X. Li, G.X. Rong, Y. Xie, L.F. Huang, C.Q. Feng, Inorg. Chem. **45**, 6404 (2006)
7. V. Subramanian, H.W. Zhu, R. Vajtai, P.M. Ajayan, B.Q. Wei, J. Phys. Chem. B. **109**, 20207 (2005)
8. S. Kirchmeyer, K. Reuter, J. Mater. Chem. **15**, 2077 (2005)
9. Y.H. Huang, J.B. Goodenough, Chem. Mater. **20**, 7237 (2008)
10. M.G. Han, S.H. Foulger, Chem. Commun. **2154** (2004)
11. A.H. Gemeay, I.A. Mansour, R.G. El-Sharkawy, A.B. Zaki, Eur. Polymer J. **41**, 2575 (2005)
12. W.R. Lee, M.G. Kim, J.R. Choi, J.I. Park, S.J. Ko, S.J. Oh, J. Cheon, J. Am. Chem. Soc. **127**, 16090 (2005)
13. X.G. Wen, S.H. Yang, Nano Lett. **2**, 451 (2002)
14. X. Wang, Y. Li, J. Am. Chem. Soc. **124**, 2880 (2002)
15. J.H. Kim, K.W. Nam, S.B. Ma, K.B. Kim, Carbon **44**, 1963 (2006)
16. M. Pourbaix, *Atlas of electrochemical equilibria in aqueous solutions, 1st English ed* (Pergamon Press, Oxford, New York, 1966), pp. 286–293
17. N. Sakmeche, J.J. Aaron, M. Fall, S. Aeiyach, M. Jouini, J.C. Lacroix, P.C. Lacaze, Chem. Commun. **2723** (1996)
18. J. Bobacka, A. Lewenstam, A. Ivaska, J. Electroanal. Chem. **489**, 17 (2000)
19. F. Jean, C. Cachet, L.T. Yu, A. Lecerf, A. Quivy, J. Appl. Electrochem. **27**, 635 (1997)
20. T. Gao, M. Glerup, F. Krumeich, R. Nesper, H. Fjellvåg, P. Norby, J. Phys. Chem. C **112**, 13134 (2008)
21. S. Garreau, G. Louarn, J.P. Buisson, G. Froyer, S. Lefrant, Macromolecules **32**, 6807 (1999)